

The thermopower and Nernst Effect in graphene in a magnetic field

Joseph G. Checkelsky and N. P. Ong

Department of Physics, Princeton University, New Jersey 08544, U.S.A.

(Dated: January 12, 2009)

We report measurements of the thermopower S and Nernst signal S_{yx} in graphene in a magnetic field H . Both quantities show strong quantum oscillations vs. the gate voltage V_g . Our measurements for Landau Levels of index $n \neq 0$ are in quantitative agreement with the edge-current model of Girvin and Jonson (GJ). The inferred off-diagonal thermoelectric conductivity α_{yx} comes close to the quantum of Amps per Kelvin. At the Dirac point ($n = 0$), however, the width of the peak in α_{yx} is very narrow. We discuss features of the thermoelectric response at the Dirac point including the enhanced Nernst signal.

In graphene, the linear dispersion of the electronic states near the chemical potential μ is well described by the Dirac Hamiltonian. As shown by Novoselov *et al.* [1, 2, 3] and by Zhang *et al.* [4, 5, 6] quantization of the electronic states into Landau Levels leads to the integer quantum Hall Effect (QHE). Because of the linear dispersion, the energy E_n of the Landau Level (LL) of index n varies as $E_n = \text{sgn}(n)\sqrt{2e\hbar v_F^2 B|n|}$, where B is the magnetic induction, v_F the Fermi velocity, e the electron charge, and \hbar is Planck's constant. The quantized Hall conductivity is given by

$$\sigma_{xy} = \frac{4e^2}{h} \left(n + \frac{1}{2} \right), \quad (1)$$

where the factor 4 reflects the degeneracy g of each LL (2 each from spin and valley degrees).

Detailed investigations of the longitudinal resistance R_{xx} and Hall resistance R_{xy} have been reported by several groups [1, 2, 3, 4, 5, 6, 7]. By contrast, the thermoelectric tensor S_{ij} is less investigated. S_{ij} relates the observed electric field \mathbf{E} to an applied temperature gradient $-\nabla T$, viz. $\mathbf{E} = \vec{\mathbf{S}} \cdot (-\nabla T)$. On the other hand, the charge current density \mathbf{J} produced by $-\nabla T$ is expressed by the thermoelectric conductivity tensor $\vec{\alpha}$, viz. $\mathbf{J} = \vec{\alpha} \cdot (-\nabla T)$. Although \mathbf{J} is not measured directly, α_{ij} may be obtained by measurements of both S_{ij} and the resistivity tensor $\rho_{ij} = R_{ij}$. (By convention, $-S_{xx}$ is the thermopower S ; we refer to $S_{yx} = E_y/|\nabla T|$ as the Nernst signal.)

A most unusual feature of the thermoelectric response of a QHE system (for $n \neq 0$) is that, despite the dominance of the off-diagonal (Hall-like) current response, the thermopower displays a large peak at each LL whereas the Nernst signal is small. In the geometry treated by Girvin and Jonson [9, 10] (Fig. 1a), the 2D sample is of finite width along $\hat{\mathbf{x}}$, but is infinite along $\hat{\mathbf{y}}$ (with the applied magnetic field $\mathbf{H} \parallel \hat{\mathbf{z}}$). As we approach either edge, the LL energy E_n rises very steeply (bold curve). At $T = 0$, edge currents I_y exist at the intersections (open circles) of E_n with the chemical potential μ . In a gradient $-\nabla T$, the magnitude of I_y is larger at the warmer edge than at the cooler edge because of increased occupation of states above μ . The difference $|\delta I_y|$ is a maximum when μ is aligned with E_n in the bulk. The correspond-

ing value of α_{yx} is then a universal quantum ($k_B e/h$) $\ln 2$ with units of Amperes per Kelvin (k_B is Boltzmann's constant). In turn, δI_y produces a quantized Hall voltage $V_H = (h/e^2)\delta I_y$ that drops $\parallel \hat{\mathbf{x}}$. Hence, conflating these 2 large off-diagonal effects, the thermopower S becomes very large when μ aligns with E_n ($n \neq 0$). By contrast, the transverse (Nernst) voltage is small (in the absence of disorder).

In graphene, this picture needs revision when μ is at the Dirac point. For the $n = 0$ LL, the nature of the edge currents is the subject of considerable debate [11, 12, 13, 14]. What are the profiles of S and S_{yx} ? We have measured S_{ij} and R_{ij} to a maximum H of 14 T at 20 and 50 K. Our results reveal that, at 9 T, the thermoelectric response in graphene already falls in the quantum regime at 50 K. The inferred off-diagonal current response α_{xy} is a series of peaks close to the quantum value ($gk_B e/h$) $\ln 2$ (independent of n , B and T). We compare our results with the calculations of Girvin and Jonson (GJ), and discuss features specific to the $n = 0$ LL at the Dirac point.

Kim and collaborators [8] have pioneered a lithographic design for measuring the thermopower of carbon nanotubes. We have adopted their approach with minor modifications for graphene. Using electron-beam lithography, we deposited narrow gold lines which serve as a micro-heater to produce $-\nabla T$ and thermometers (Fig 1d). The latter are also used as current leads when R_{xx} and R_{xy} are measured. Above 10 K, the thermometers can resolve $\delta T \sim \pm 1$ mK. The typical δT is ~ 10 mK between the 2 thermometers. However, the small spacing of the voltage leads ($\sim 2 \mu\text{m}$) leads to an uncertainty of $\pm 10\%$ in estimating δT between them. A slowly oscillating current at frequency ω is applied to the heater and the resulting thermoelectric signals are detected at 2ω and -90° out of phase.

In our geometry with $-\nabla T \parallel \hat{\mathbf{x}}$, $\mathbf{H} \parallel \hat{\mathbf{z}}$, the charge current density \mathbf{J} is (summation over repeated indices implied)

$$J_i = \sigma_{ij} E_j + \alpha_{ij} (-\partial_j T) \quad (i = x, y). \quad (2)$$

The (2D) conductivity and thermoelectric conductivity tensors are often written as $\sigma_{ij} = L_{ij}^{11}(e^2/T)$ and $\alpha_{ij} = L_{ij}^{12}/T^2$, respectively. Setting $\mathbf{J} = 0$, we have for the

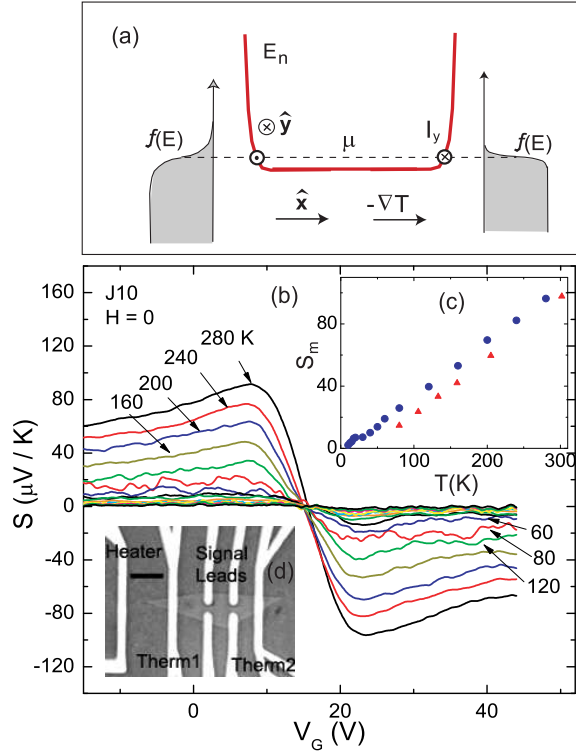


FIG. 1: (Color online) (Panel a) The effect of $-\nabla T$ on the edge currents I_y in a QHE system ($n \neq 0$). The energy E_n of a LL (bold curve) increases very steeply at the sample edges, with μ the chemical potential (dashed line). If $H_z > 0$, I_y is negative (positive) at the left (right) edge, as indicated by open circles. The magnitude $|I_y|$ is larger at the warmer edge. Fermi-Dirac distributions $f(E)$ are sketched at the sides. (Panel b) Curves of thermopower $S = -S_{xx}$ vs. gate voltage V_g in Sample J10 at selected T . The curves are antisymmetric about the Dirac Point which occurs at the offset voltage $V_0 = 15.5$ V. The peak value S_m is nominally linear in T from 25 to 300 K (Panel c). Less complete data from sample K59 are also plotted. A photo of Sample J10 (faint polygon) is shown in Panel (d). A micro-heater as well as thermometers (therm) and signal leads are patterned with electron-beam lithography. The black scale bar is $3 \mu\text{m}$.

observed E -fields

$$E_i = -\rho_{ik}\alpha_{kj}(-\partial_j T) = S_{ij}(-\partial_j T), \quad (3)$$

with $\rho_{ij} = R_{ij}$ the 2D resistivity tensor. The thermopower $S = -E_x/|\nabla T|$ equals $\rho_{xx}\alpha_{xx} + \rho_{yx}\alpha_{xy}$ ($S > 0$ for hole doping), while the Nernst signal is given by (with $\rho_{xx} = \rho_{yy}$)

$$S_{yx} = \rho_{xx}\alpha_{xy} - \rho_{yx}\alpha_{xx}. \quad (4)$$

The 2 terms tend to cancel mutually, except at the Dirac point where ρ_{yx} vanishes (see below).

Inverting Eq. 3, we may calculate the tensor α_{ij} from measured quantities. We have

$$\begin{aligned} \alpha_{xx} &= -(\sigma_{xx}E_x + \sigma_{xy}E_y)/|\nabla T| \\ \alpha_{xy} &= (-\sigma_{xy}E_x + \sigma_{xx}E_y)/|\nabla T|. \end{aligned} \quad (5)$$

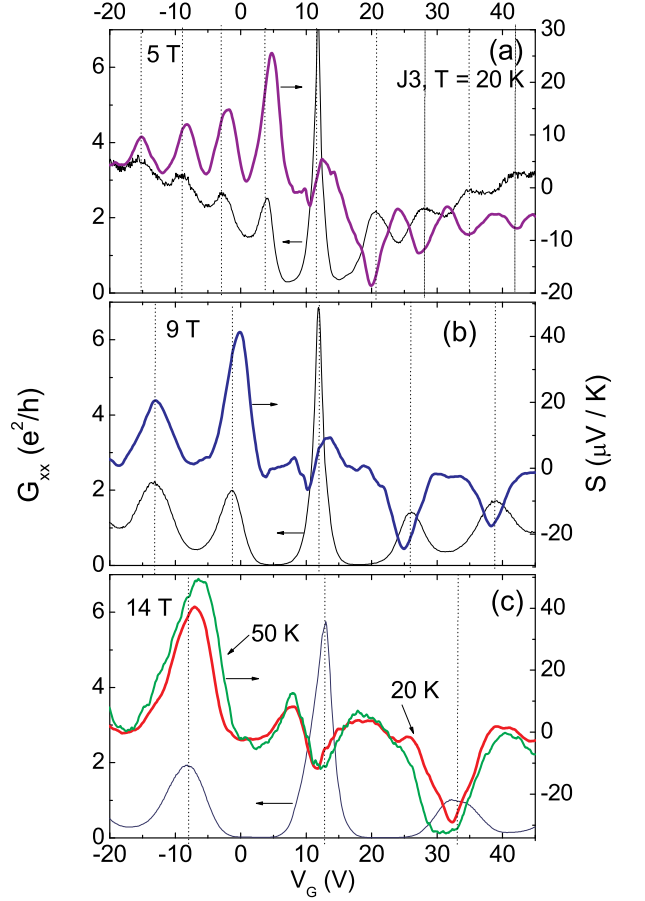


FIG. 2: (Color online) Variation of thermopower S vs. V_g (bold curves) and conductance G_{xx} vs. V_g (thin curves) in Sample J3 at $H = 5, 9$ and 14 T (Panels a, b and c, respectively). The offset $V_0 = 12.5$ V. All curves were measured at 20 K except for the curve at 50 K in Panel (c). Vertical lines locate the maxima of G_{xx} .

Under field reversal ($\mathbf{H} \rightarrow -\mathbf{H}$), S is symmetric whereas S_{yx} is antisymmetric. For each curve taken in field, we repeat the measurement with \mathbf{H} reversed. All curves of S and S_{yx} reported here have been (anti)symmetrized with respect to \mathbf{H} . As for charge-inversion symmetry, we expect the sign of S to change with the shifted gate voltage $V'_g \equiv V_g - V_0$ (i.e. between hole and electron filling), but the sign of S_{yx} stays unchanged (V_0 is the offset voltage). However, we have not imposed charge-inversion symmetrization constraints on the curves. Apart from field (anti)symmetrization, all the curves are the raw data.

Figure 1b shows traces of S vs. V_g at selected T . The thermopower S changes sign as V_g crosses the charge-neutral point (Dirac Point), assuming positive (negative) values on the hole (electron) side. The peak value S_m is nominally T -linear from ~ 20 K to 300 K (Fig. 1c).

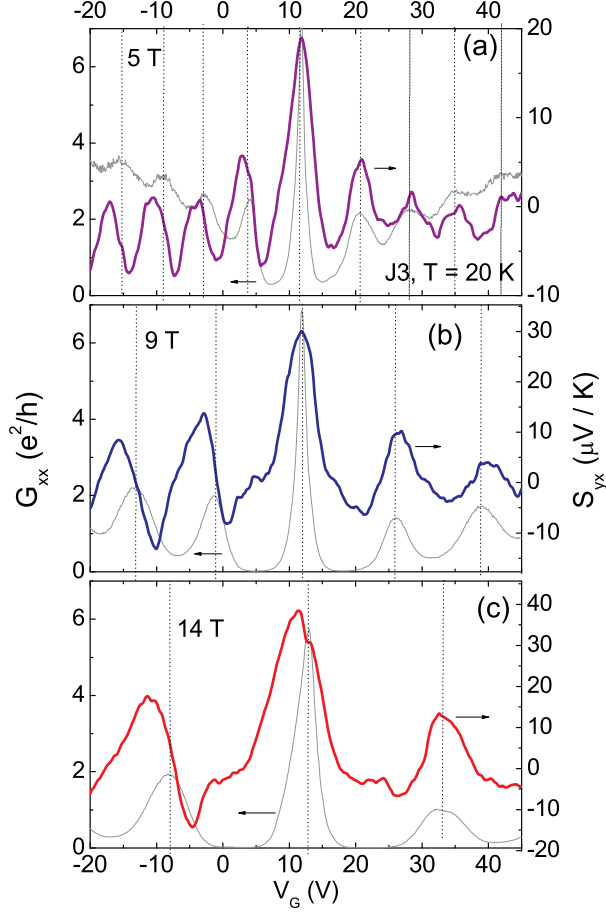


FIG. 3: (Color online) Variation of Nernst signal S_{yx} vs. V_g (bold curves) and conductance G_{xx} vs. V_g (thin curves) in J3 at the 3 field values $H = 5, 9$ and 14 T (Panels a, b and c, respectively). All curves were measured at 20 K. Vertical lines locate the maxima of G_{xx} . The sign of S_{yx} was incorrectly assigned in a previous version of this paper [15].

In sharp contrast to the smooth variation in Fig. 1, the curves of S vs. V_g show pronounced oscillations when H is finite, reflecting Landau quantization of the Dirac states. Figures 2a, b and c display S vs. V_g (bold curves) with H fixed at the values $5, 9$ and 14 T, respectively. For comparison, we have also plotted (as thin curves) the corresponding conductance $G_{xx} = \sigma_{xx}$. (With the exception of the curve at 50 K in Panel (c), all curves were measured at 20 K.) Whereas at large $|n|$, the peaks in S are aligned with those in G_{xx} (vertical lines), at $n = \pm 1$, they disagree. In Panel a, the peaks for $V_g' < 0$ (hole doping) decrease systematically in magnitude as n increases from 1 to 4.

The curves of the Nernst signal S_{yx} are displayed in Fig. 3. For $n \neq 0$, S_{yx} displays a dispersive profile centered at the vertical lines, in contrast with the peak

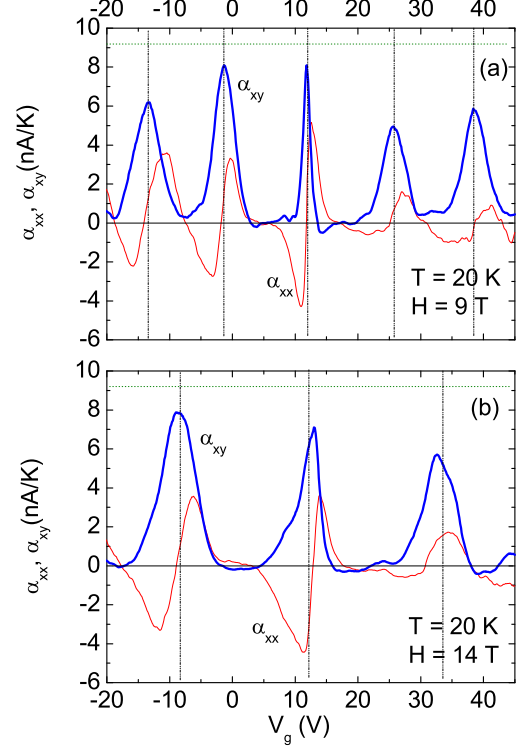


FIG. 4: (Color online) The thermoelectric response functions α_{xx} (faint curve) and α_{xy} (bold) vs. V_g at 9 T (Panel a) and 14 T (b) at $T = 20$ K calculated from S and S_{yx} (Eq. 5). In (a), the width of the peak at $n=0$ is narrower than the others by a factor of 5. In both panels, vertical lines locate the peaks of G_{xx} . The horizontal dashed line is $(4k_B e/h) \ln 2$.

profiles of S . Moreover, S_{yx} is smaller in magnitude by a factor of 4-5. For the $n = 0$ LL, however, the profiles change character, with S_{yx} displaying a large positive peak. The reason for the enhancement of S_{yx} at the Dirac point is discussed below. The positive sign of S_{yx} at the $n=0$ LL implies that the Nernst E -field \mathbf{E}_N is parallel to $\mathbf{H} \times (-\nabla T)$ [15].

In the theory of GJ [9], valid for GaAs-based devices, the edge current difference is $\delta I_y = (ge/h) \sum_n \int dk (\partial \epsilon / \partial k) (\partial f / \partial T) \delta T$, with $f(\epsilon)$ the Fermi-Dirac distribution. The off-diagonal term α_{xy} is given by $(e/hT) \sum_n \int_{E_n}^{\infty} d\epsilon (\epsilon - \mu) \left(-\frac{\partial f}{\partial \epsilon} \right)$. When $\mu = E_n$, α_{xy} attains a peak value, corresponding to a quantized current per Kelvin, given by ($g=1$)

$$\alpha_{xy}^{max} = \frac{k_B e}{h} \ln 2 \quad (\sim 2.32 \text{ nA/K}). \quad (6)$$

GJ find that S displays a series of peaks, with the peak

value at LL n given by

$$S_{peak}(n) = \frac{k_B}{e} \frac{\ln 2}{(n + \frac{1}{2})}. \quad (7)$$

At low T , S is independent of H and T .

In Fig. 2, the peak value of S at the $n = -1$ LL increases from 25 at 5 T to 41 $\mu\text{V}/\text{K}$ at both 9 and 14 T. Moreover, as T increases from 20 to 50 K (Panel c), the peak increases only weakly (41 to 48 μV) in sharp contrast with the T -linear behavior at $H=0$ (Fig. 1, inset). We thus confirm the prediction of GJ that S (at the peak) saturates to a value independent of T and H at sufficiently low T . This saturation contrasts with the T -linear behavior of S in $H=0$ (Fig. 1c).

In graphene, however, Berry phase effects lead to a the $\frac{1}{2}$ -integer shift in Eq. 1 [4]. In evaluating $\sigma_{xy} \sim \sum_n f(E_n)$, the $\frac{1}{2}$ -integer shift implies that $S_{peak}(n)$ decreases as $k_B \ln 2/(en)$, instead of Eq. 7. The measured values $S_{peak} = 41 \mu\text{V}/\text{K}$ at $n = -1$ at 9 T already exceeds slightly the predicted value 39.7 $\mu\text{V}/\text{K}$ in Eq. 7. Future experiments on cleaner samples may yield values closer to the predicted value 59.6 $\mu\text{V}/\text{K}$ for Dirac systems. Regardless, for LL with $n \neq 0$, our observations are generally consistent with the GJ theory. In principle, Eq. 7 provides a way to measure δT on micron-scales with a resolution approaching voltage measurements.

The most interesting question is the thermoelectric response of the $n=0$ LL. This is easier to analyze using the pure thermoelectric currents α_{xx} and α_{xy} (obtained using Eqs. 5). In Fig. 4a, α_{xy} and (α_{xx}) is plotted as bold (thin) curves for $H=9$ T and $T = 20$ K. Panel (b) shows the curves at 14 T. Compared with S vs. V_g , the peaks in α_{xy} are much narrower and clearly separated by intervals in which α_{xy} is nominally zero. Likewise, the purely dispersive profile of α_{xx} is also more apparent. Consistent with the GJ theory, the overall magnitude of α_{xy} (for $n \neq 0$) is larger than that of α_{xx} .

A striking feature of α_{xy} is that its peaks are independent of n . Their average value ~ 75 nA/K reaches to

within 30% of the quantized value of Eq. 6 with $g = 4$ (horizontal dashed line). The largest uncertainty in our measurement is in estimating the gradient between the voltage leads. For the $n = 0$ LL, the shortfall may also reflect incipient splitting of the Landau sublevels (compare 9 and 14 T traces). The uniformity of the peaks in α_{xy} accounts for the observed enhancement of the Nernst peak at the Dirac point. By Eq. 4, S_{yx} is the difference of 2 positive terms. For $n \neq 0$, the 2 terms are matched, and the partial cancellation leads to a dispersive profile. However, for $n = 0$, the vanishing of ρ_{yx} as $V_g' \rightarrow 0$ strongly suppresses the second term $-\rho_{yx}\alpha_{xx}$. The remaining term $\rho_{xx}\alpha_{xy}$ then dictates the size and profile of the Nernst peak.

We note that the sign of α_{xy} is a direct consequence of the edge-currents [9]. When $H_z > 0$, $I_y < 0$ on the warmer edge and $I_y < 0$ on the cooler edge, as depicted in Fig. 1a. As a result, $\alpha_{xy} > 0$ for both hole-and electron-doping.

Our measurements are consistent with the GJ theory for $n \neq 0$. For the $n=0$ LL, however, there is considerable uncertainty about the nature of the edge states in graphene (or whether they exist in large H). The simple edge-current picture for understanding the peaks in α_{xy} may need significant revision for $n = 0$, despite the similarity of the peak magnitude. We also note that the peak at $n = 0$ is much narrower (by a factor of 5) than the other peaks. This is also not understood. By going to cleaner samples and higher fields, we hope to exploit this narrow width to resolve splitting of the 4 sublevels at $n = 0$.

We are grateful to P. A. Lee for many discussions. The research is supported by NSF through a MRSEC grant (DMR-0819860).

Note added After we completed these experiments, we learned of 2 thermopower and Nernst experiments on graphene posted recently (Yuri M. Zuev *et al.*, cond-mat arXiv: 0812.1393 and Peng Wei *et al.*, cond-mat arXiv: 0812.1411).

-
- [1] K. S. Novoselov *et al.* Science **306**, 666-669 (2004).
[2] K. S. Novoselov *et al.* Proc. Natl. Acad. Sci. USA **102**, 10451-10453 (2005).
[3] K. S. Novoselov *et al.* Nature **438**, 197-200 (2005).
[4] Y. Zhang, J. Tan, H. L. Stormer and P. Kim, Nature **438**, 201-204 (2005).
[5] Y. Zhang *et al.* Phys. Rev. Lett. **96**, 136806 (2006).
[6] Z. Jiang, Y. Zhang, H. L. Stormer and P. Kim, Phys. Rev. Lett. **99**, 106802 (2007).
[7] Joseph G. Checkelsky, Lu Li, and N. P. Ong, Phys. Rev. Lett. **100**, 206801 (2008).
[8] J.P. Small, K.M. Perez, and P. Kim, Phys. Rev. Lett. **91**, 256801 (2003).
[9] S. M. Girvin and M. Jonson, J. Phys. C: Solid State Phys. **15**, L1147 (1982).
[10] M. Jonson and S. M. Girvin, Phys. Rev. B **29**, 1939 (1984).
[11] H. A. Fertig and L. Brey, Phys. Rev. Lett. **97**, 116805 (2006).
[12] D. A. Abanin, P. A. Lee and L. S. Levitov, Phys. Rev. Lett. **96**, 176803 (2006).
[13] K. Nomura and A. H. MacDonald, Phys. Rev. Lett. **96**, 256602 (2006).
[14] D. A. Abanin *et al.* Phys. Rev. Lett. **98**, 196806 (2007).
[15] In a previous posted version of this manuscript (cond-mat arXiv:0812.2866.v1), the sign of S_{yx} was incorrectly assigned. After careful checking and further measurements, we have determined that $S_{yx} > 0$ and $\alpha_{xy} > 0$ at $n = 0$ as reported here. The sign of E_y is the same as that for the vortex-Nernst effect in superconductors.